

Optimal Beamforming Structure and Efficient Optimization Algorithms for Generalized Multi-Group Multicast Beamforming Optimization

Tianyu Fang, Yijie Mao, *Member, IEEE*

Abstract—In this work, we focus on solving non-smooth non-convex maximization problems in multi-group multicast transmission. Leveraging Karush-Kuhn-Tucker (KKT) optimality conditions and successive incumbent transcending (SIT) duality, we thoroughly analyze the optimal beamforming structure for a set of optimization problems characterized by a general utility-based objective function. By exploiting the identified optimal structure, we further unveil inherent low-dimensional beamforming structures within the problems, which are asymptotically optimal in various regimes of transmit signal-to-noise ratios (SNRs) or the number of transmit antennas. Building upon the discovered optimal and low-dimensional beamforming structures, we then propose highly efficient and toolbox-free optimization algorithms to solve a specific multi-group multicast optimization problem based on the weighted sum rate (WSR) utility function. The proposed algorithms first use the cyclic maximization (CM) framework to decompose the problem into multiple subproblems, each has an optimal or low-dimensional closed-form beamforming solution structure. Then, we propose the projected adaptive gradient descent (PAGD) algorithm to compute the optimal Lagrangian dual variables for each subproblem. Numerical results show that the proposed algorithms maintain comparable or improved WSR performance compared to baseline algorithms, while dramatically reducing the computational complexity. Notably, the proposed ultra-low-complexity algorithms based on low-dimensional beamforming structures achieve near optimal WSR performance with extremely low computational complexity. This complexity remains independent of the number of transmit antennas, making them promising and practical for extremely large multiple-input multiple-output (XL-MIMO) applications in 6G.

Index Terms—Multi-group multicast, transmit beamforming optimization, weighted sum-rate maximization, optimal beamforming structure.

I. INTRODUCTION

Wireless communication systems are continually advancing to fulfill the escalating demands for high data rates, reliability, and energy efficiency. Within this landscape, the application of multicast strategies is crucial to effectively meet the communication requirements of numerous users seeking simultaneous access to identical data. Physical-layer multicast beamforming was first proposed in [1] and has drawn much attention in recent years for its potential to support multi-group multicasting in various wireless services and applications, such as videoconferencing, mobile commerce, and intelligent

transportation systems. With the emerging extremely large-scale multiple-input multiple-output (XL-MIMO) for 6G [2], it is vital to develop low-complexity multi-group multicast beamforming solutions to address the high computational demands of these large-scale systems.

The design of transmit beamforming in wireless communication systems aims to improve spectral or energy efficiency, typically involving the following two types of optimization problems: 1) total transmit power minimization under minimum signal-to-interference-and-noise ratio (SINR) constraints for all user—the *quality of service (QoS) problem*; 2) the system utility maximization subject to a total transmit power constraint—the *utility problem*. These two types of problems are interconnected, and solutions to one can provide insight into the other. However, in multi-group multicast transmission, these two problems are generally NP-hard even in single-group scenarios [1]. Various algorithms have been proposed to address multicast beamforming problems, including globally optimal and suboptimal algorithms. In [3], a globally optimal beamforming optimization algorithm employing the branch and bound (BB) method has been proposed for the QoS problem. Although this global optimal algorithm exhibits attractive performance, it is tailored to a single-group scenario and is hindered by high computational complexity. Therefore, state-of-the-art work focuses primarily on developing suboptimal algorithms capable of achieving near-optimal performance.

Among the suboptimal algorithms for solving multicast beamforming problems, semi-definite relaxation (SDR) [1], [4]–[7] stands out as a popular convex relaxation (CR)-based method that achieves a near-optimal solution. However, as the size of the multicast network increases, the performance of SDR degrades quickly and the computational complexity increases sharply due to the auxiliary relaxation variables. To address these drawbacks, another category of optimization algorithms based on the convex approximation (CA) has emerged and received extensive investigation. Algorithms utilizing various techniques, including successive convex approximation (SCA), [8]–[10], weighed minimum mean square error (WMMSE) [11], [12], fractional programming (FP) [13], [14], and majorization-minimization (MM) [15], [16], have been proposed to solve various multi-group multicast beamforming optimization problems. Generally speaking, these CA-based algorithms are mathematically equivalent and share the same ability to find a near-optimal solution for the original problem [17]. All the aforementioned algorithms either transform the original non-convex problem into a high-dimensional block-wise convex problem (i.e., WMMSE and FP) or construct a sequence of convex surrogate functions at a given point (i.e.,

This work has been supported in part by the National Nature Science Foundation of China under Grant 62201347; and in part by Shanghai Sailing Program under Grant 22YF1428400.

T. Fang and Y. Mao are with the School of Information Science and Technology, ShanghaiTech University, Shanghai 201210, China (e-mail: {fangty, maoyj}@shanghaitech.edu.cn).

SCA and MM). And each convex subproblem is solved using standard interior-point method (IPM), typically implemented by a dedicated solver in optimization toolboxes, such as CVX [18]. However, the practical use of these algorithms is hampered by the undesirable computational complexity resulting from the iterative use of CVX optimization solvers.

To further reduce the computational complexity, several approaches shift towards closed-form and low-complexity beamforming designs for each convex subproblem obtained from the CA-based methods. Specifically, for the smooth QoS problems, alternating direction method of multipliers (ADMM) [19] and extragradient-based [20] algorithms have been proposed to solve each subproblem. For the non-smooth utility problems, subgradient-based [21] and log-sum-exp (LSE)-based [15] algorithms have been introduced to handle each non-smooth subproblem. These methods generally offer lower complexity than the CVX-based algorithms. However, with the advent of XL-MIMO, which further boosts the number of transmit antennas by at least an order of magnitude compared to massive MIMO (e.g., several hundred or even thousands of transmit antennas), the computational complexity of these approaches still grows sharply with the number of transmit antennas. While certain low-complexity beamforming approaches, such as zero-forcing (ZF) [22] and weighted maximum ratio transmission (MRT) [23], are employed to reduce the dimension of the optimization problem, a unified analysis of the conditions under which these beamforming techniques are effective is currently lacking.

The aforementioned ZF and MRT low-complexity beamforming approaches originate from the optimal beamforming structure [24]–[26]. For unicast-only transmission, the optimal beamforming structure was identified in [24] for both QoS and general utility problems. It was demonstrated in [24] that the optimal beamforming structures for these two problem types are equivalent. For multi-group multicast transmission, the optimal beamforming structure was identified in [25], with a particular focus on the QoS and max-min fair (MMF) problems. Building upon the optimal multi-group multicast beamforming structure identified in [25], some ultra-low-complexity algorithms [20], [27], [28] are proposed for large-scale communication networks. However, these algorithms mainly focus on addressing the QoS problem or its inverse MMF problem by iteratively solving the QoS problem via a bisection search. This approach is not applicable for solving the utility problem due to the potentially high-dimensional search. To the best of our knowledge, the optimal multi-group multicast beamforming structure for the generalized utility function-based maximization problems has not yet been identified. Additionally, efficient algorithms for directly solving these non-convex non-smooth problems with popular utility functions, such as weighted sum rate (WSR), geometric mean or harmonic mean of group rates are yet to be explored.

This paper aims to bridge this gap by discovering the optimal multi-group multicast beamforming structure and efficient algorithms for solving the generalized utility function maximization problems. The key contributions of this paper are outlined as follows:

- *A thorough analysis of the optimal multi-group multicast*

beamforming structure: By leveraging the Karush-Kuhn-Tucker (KKT) optimality conditions and the successive incumbent transcending (SIT) duality [29], we identify the optimal multi-group multicast beamforming structure for a generalized utility function-based maximization problem. In contrast to the approach in [25], our method first derives out the optimal solution directly through the first-order optimality conditions of the original QoS problem. We then establish the SIT duality between the QoS problem and the utility problem, revealing the multi-group multicast beamforming for both types of problems shares the same optimal structure.

- *A comprehensive exploration of low-dimensional beamforming structures:* The revealed optimal beamforming structure provides valuable insights into the multi-group multicast beamforming design. This inspires us to explore inherent low-dimensional beamforming structures that are asymptotically optimal in various regimes of transmit signal-to-noise (SNR) or the number of transmit antennas. These low-dimensional beamforming structures are particularly beneficial in reducing the computational complexity of beamforming design, especially in XL-MIMO systems.
- *Development of highly efficient and optimization toolbox-free algorithms based on the identified beamforming structures:* Leveraging the identified optimal and low-complexity beamforming structures, we propose highly efficient and optimization toolbox-free algorithms to solve the non-smooth utility problem. Specifically, we first propose to utilize the cyclic maximization (CM) framework to decompose the problem into multiple subproblems, each has an optimal or low-dimensional closed-form beamforming solution structure. Then, the projected adaptive gradient descent (PAGD) algorithm is proposed to compute the optimal Lagrangian dual variables for each subproblem.
- Numerical simulations demonstrate the superior efficiency of the proposed algorithms, as evidenced by their low central processing unit (CPU) time consumption, all while maintaining comparable or improved WSR performance compared to existing optimization algorithms. Surprisingly, the proposed ultra-low-complexity algorithms, leveraging low-dimensional beamforming structures, attain near-optimal WSR performance with remarkably low computational complexity. Importantly, this complexity remains independent of the number of transmit antennas, making them promising and practical for extensive applications in 6G, particularly in XL-MIMO scenarios.

Organization: The rest of this paper is organized as follows. Section II and Section III provide thorough analysis of the optimal and low-complexity multi-group multicast beamforming structures, respectively, for the generalized utility problem. In Section IV, we leverage the CM framework and Lagrange duality to derive closed-form solution for each convex subproblem. Simulation results are presented in Section V. In the end, Section VI concludes the paper.

Notations: Vectors and matrices are represented by bold

lower-case and upper-case letters, respectively. The complex space is denoted by \mathbb{C} , the real space by \mathbb{R} , and \mathbb{R}_+ denotes the set of real values larger than 0. Expectation over a random variable s is denoted as $\mathbb{E}[s]$. The magnitude of a complex number x is expressed as $|x|$. The circularly symmetric complex Gaussian distribution (CSCG) with zero mean and variance σ^2 is denoted as $\mathcal{CN}(0, \sigma^2)$. The conjugate transpose is represented by $(\cdot)^H$. The optimal solution for a convex subproblem is denoted as $(\cdot)^*$. The local and global optimal solutions for the original non-convex problem are represented by $(\cdot)^\diamond$ and $(\cdot)^\circ$, respectively. $\text{diag}\{\mathbf{y}\}$ denotes a diagonal matrix with the entries of \mathbf{y} along the main diagonal, and $\text{blkdiag}\{\mathbf{y}_1, \dots, \mathbf{y}_N\}$ is block-diagonal matrix with vector or matrices $\{\mathbf{y}_1, \dots, \mathbf{y}_N\}$ along its main diagonal.

II. OPTIMAL MULTI-GROUP MULTICAST BEAMFORMING STRUCTURE

A. System Model and Problem Formulation

Consider a downlink multi-group multicast wireless communication network, where a base station (BS) equipped with L antennas simultaneously serving G non-overlapping user groups indexed by $\mathcal{G} = \{1, \dots, G\}$. In each user group g , there are K_g single-antenna users indexed by $\mathcal{K}_g = \{1, \dots, K_g\}, \forall g \in \mathcal{G}$. The total number of users in the system is $K = \sum_{g=1}^G K_g$. All users within the same group g require the same multicast stream s_g . Without loss of generality, the transmit data stream vector $\mathbf{s} = [s_1, \dots, s_G]^T$ is assumed to have zero mean and identity variance, i.e., $\mathbb{E}\{\mathbf{s}\mathbf{s}^H\} = \mathbf{I}_G$. Let $\mathbf{w}_g \in \mathbb{C}^{L \times 1}$ be the corresponding beamforming vector for the stream $s_g, \forall g \in \mathcal{G}$, the transmitted signal at the BS is $\sum_{g=1}^G \mathbf{w}_g s_g$. The total transmit power is required to be less than or equal to the upperbound P_t , i.e., $\sum_{g=1}^G \|\mathbf{w}_g\|^2 \leq P_t$.

Let $\mathbf{h}_{gk}^H \in \mathbb{C}^{1 \times L}$ be the channel vector from the BS to the user k in group $g, \forall k \in \mathcal{K}_g, \forall g \in \mathcal{G}$, the signal received at user k in group g is expressed as

$$y_{gk} = \mathbf{h}_{gk}^H \sum_{i=1}^G \mathbf{w}_i s_i + n_{gk}, \forall k \in \mathcal{K}_g, \forall g \in \mathcal{G}, \quad (1)$$

where $n_{gk} \sim \mathcal{CN}(0, \sigma_{gk}^2)$ denotes the additive white Gaussian noise (AWGN) at user k in group g with σ_{gk}^2 denoting the noise power.

Each user in group g decodes the intended multicast stream s_g with the SINR of

$$\gamma_{gk} = |\mathbf{h}_{gk}^H \mathbf{w}_g|^2 \left(\sum_{i=1, i \neq g}^G |\mathbf{h}_{gk}^H \mathbf{w}_i|^2 + \sigma_{gk}^2 \right)^{-1}, \forall k \in \mathcal{K}_g, \forall g \in \mathcal{G}. \quad (2)$$

Consequently, the achievable rate for the multicast stream s_g is

$$R_g = \min_{k \in \mathcal{K}_g} \{\log(1 + \gamma_{gk})\}, \forall g \in \mathcal{G}. \quad (3)$$

In this study, our primary focus is on addressing a highly generalized multi-group multicast beamforming optimization problem, characterized by an utility function denoted as $f(R_1, \dots, R_G)$. Following [24], we assume that $f(\cdot)$ is a continuous, strictly increasing function concerning the achievable

SINRs of each user. It should be the operations that preserve concavity, such as non-negative weighted sums, pointwise minimum, and so on. The generalized utility problem for multi-group multicast transmission is formulated as

$$\mathcal{U} : \max_{\mathbf{W}} f(R_1, \dots, R_G) \quad (4a)$$

$$\text{s.t. } \text{Tr}(\mathbf{W}\mathbf{W}^H) \leq P_t, \quad (4b)$$

where $\mathbf{W} \triangleq [\mathbf{w}_1, \dots, \mathbf{w}_G]$. This problem poses two major challenges: the presence of multiple non-convex fractional SINR expressions (2) and the non-smooth nature of the achievable rate expressions (3) for multicast streams. Notably, the multicast beamforming design is inherently NP-hard, even when the problem (4) is reduced to the single-group setting where inter-group interference is absent [1].

To address the non-smooth characteristics of problem (4), we first investigate the more tractable QoS problem in (5), and subsequently extend the findings to problem (4) by exploring their interrelations. The QoS problem is formulated as follows

$$\mathcal{P} : \min_{\mathbf{W}} \text{Tr}(\mathbf{W}\mathbf{W}^H) \quad (5a)$$

$$\text{s.t. } \gamma_{gk} \geq \alpha_g, \forall k \in \mathcal{K}_g, \forall g \in \mathcal{G}, \quad (5b)$$

where α_g refers to the QoS threshold for multicast stream s_g . Users within the same group share a common QoS threshold since the achievable rate is constrained by the worst-case user within each user group. This differs from the unicast-only scenario, where each user has an individual QoS threshold. Problem (5) has been proven to be non-convex and NP-hard [4].

In the next subsections, we focus on identifying the optimal multicast beamforming structure for both problem (4) and problem (5), using an approach different from the iterative SCA method in [25].

B. Optimal Multicast Beamforming Structure for QoS problem

In this subsection, we identify the optimal multicast beamforming structure for the power minimization problem (5). Specifically, we begin by using Lemma 1 to show that the KKT conditions of (5) are necessary conditions for all stationary points. Following this, we directly unveil the optimal beamforming structure of (5) based on its KKT conditions.

Lemma 1. *Linear independence constraint qualification (LICQ) [30] holds for problem (5) when all channel vectors $\{\mathbf{h}_{gk}, \forall k \in \mathcal{K}_g, \forall g \in \mathcal{G}\}$ are linearly independent.*

Proof: Constraint (5b) can be rewritten as

$$\underbrace{\sum_{i=1, i \neq g}^G \frac{1}{\sigma_{gk}^2} |\mathbf{h}_{gk}^H \mathbf{w}_i|^2 + 1}_{c_{gk}(\mathbf{W})} - \frac{1}{\alpha_g \sigma_{gk}^2} |\mathbf{h}_{gk}^H \mathbf{w}_g|^2 \leq 0. \quad (6)$$

Denote the left-hand side of (6) as $c_{gk}(\mathbf{W})$, then the gradient of $c_{gk}(\mathbf{W})$ with respect to \mathbf{W} is given as

$$\nabla c_{gk}(\mathbf{W}) = \frac{2}{\sigma_{gk}^2} \mathbf{h}_{gk} \mathbf{h}_{gk}^H \left[\mathbf{w}_1, \dots, \frac{-1}{\alpha_g} \mathbf{w}_g, \dots, \mathbf{w}_G \right].$$

All gradients $\{\nabla c_{gk}(\mathbf{W}), \forall k \in \mathcal{K}_g, \forall g \in \mathcal{G}\}$ are linearly independent and therefore satisfy LICQ if the channel vectors $\{\mathbf{h}_{gk}, \forall k \in \mathcal{K}_g, \forall g \in \mathcal{G}\}$ exhibit linear independence. ■

Remark 1. The power minimization problem (5) for multi-group multicasting beamforming would be infeasible when the channel vectors from different groups are linearly dependent, since the interference from other groups can not be eliminated by the beamforming vectors. Without loss of generality, we assume that all channel vectors $\{\mathbf{h}_{gk}\}$ are linearly independent, and therefore problem (5) is feasible. This assumption holds for widely adopted channel models, such as Rayleigh fading.

Lemma 1 implies that the KKT conditions are necessary conditions for any stationary point for problem (5). Therefore, we are able to analyze the problem (5) using the KKT optimality conditions. By introducing a set of Lagrange multipliers $\{\lambda_{gk}\}$ for the corresponding reformulated SINR constraints (6), we define the Lagrangian function of (5) as

$$\mathcal{L}_{(5)}(\mathbf{W}, \boldsymbol{\lambda}) = \frac{1}{2} \sum_{g=1}^G \|\mathbf{w}_g\|^2 + \frac{1}{2} \sum_{g=1}^G \sum_{k=1}^{K_g} \lambda_{gk} \left(\sum_{i=1, i \neq g}^G \frac{1}{\sigma_{gk}^2} |\mathbf{h}_{gk}^H \mathbf{w}_i|^2 + 1 - \frac{1}{\alpha_g \sigma_{gk}^2} |\mathbf{h}_{gk} \mathbf{w}_g|^2 \right),$$

where $\boldsymbol{\lambda} \triangleq [\boldsymbol{\lambda}_1, \dots, \boldsymbol{\lambda}_G]$ with $\boldsymbol{\lambda}_g = [\lambda_{g1}, \dots, \lambda_{gK_g}]^T$. The first-order derivative of $\mathcal{L}_{(5)}(\mathbf{W}, \boldsymbol{\lambda})$ with respect to \mathbf{w}_g is given by

$$\frac{\partial \mathcal{L}_{(5)}}{\partial \mathbf{w}_g} = \mathbf{w}_g + \sum_{i \neq g}^G \sum_{k=1}^{K_i} \frac{\lambda_{ik}}{\sigma_{ik}^2} \mathbf{h}_{ik} \mathbf{h}_{ik}^H \mathbf{w}_g - \sum_{k=1}^{K_g} \frac{\lambda_{gk}}{\alpha_g \sigma_{gk}^2} \mathbf{h}_{gk} \mathbf{h}_{gk}^H \mathbf{w}_g. \quad (7)$$

Therefore, for any stationary point \mathbf{W}^\diamond of problem (5), there exists a set of Lagrange multipliers $\{\lambda_{gk}^\diamond\}$ satisfying the stationary conditions, i.e., $\partial \mathcal{L}_{(5)} / \partial \mathbf{w}_g^\diamond = \mathbf{0}$, which leads to

$$\left(\mathbf{I}_L + \sum_{i=1}^G \sum_{k=1}^{K_i} \frac{\lambda_{ik}^\diamond}{\sigma_{ik}^2} \mathbf{h}_{ik} \mathbf{h}_{ik}^H \right) \mathbf{w}_g^\diamond = \sum_{k=1}^{K_g} \frac{\lambda_{gk}^\diamond}{\sigma_{gk}^2} \left(1 + \frac{1}{\alpha_g} \right) \mathbf{h}_{gk} \mathbf{h}_{gk}^H \mathbf{w}_g^\diamond. \quad (8)$$

Equation (8) is obtained from (7) by adding and subtracting the term $\sum_{k=1}^{K_g} \frac{\lambda_{gk}^\diamond}{\sigma_{gk}^2} \mathbf{h}_{gk} \mathbf{h}_{gk}^H \mathbf{w}_g^\diamond$, and then setting it to zero. The derived locally optimal beamforming solution is given as

$$\mathbf{w}_g^\diamond = \left(\mathbf{I}_L + \sum_{i=1}^G \sum_{k=1}^{K_i} \frac{\lambda_{ik}^\diamond}{\sigma_{ik}^2} \mathbf{h}_{ik} \mathbf{h}_{ik}^H \right)^{-1} \sum_{k=1}^{K_g} \frac{\lambda_{gk}^\diamond}{\sigma_{gk}^2} \left(1 + \frac{1}{\alpha_g} \right) \mathbf{h}_{gk} \mathbf{h}_{gk}^H \mathbf{w}_g^\diamond. \quad (9)$$

The global-optimal beamforming solution of problem (5) aligns with the beamforming structure in (9), as it belongs to one of the local-optimal solutions of (5). For simplicity, we write out the optimal beamforming structure in matrix form as shown in the following Theorem 1.

Theorem 1. The optimal multi-group multicast beamforming structure for problem (5) is

$$\mathbf{w}_g^\diamond = \left(\mathbf{I}_L + \sum_{i=1}^G \mathbf{H}_i \boldsymbol{\Theta}_i^\diamond \mathbf{H}_i^H \right)^{-1} \mathbf{H}_g \mathbf{d}_g^\diamond, \forall g \in \mathcal{G}, \quad (10)$$

where $\mathbf{H}_i \triangleq [\mathbf{h}_{i1}, \dots, \mathbf{h}_{iK_i}]$, $\boldsymbol{\Theta}_i^\diamond \triangleq \text{diag}\{\theta_{i1}^\diamond, \dots, \theta_{iK_i}^\diamond\}$ with $\theta_{ik}^\diamond = \frac{\lambda_{ik}^\diamond}{\sigma_{ik}^2}$, $\mathbf{d}_g^\diamond \triangleq [d_{g1}^\diamond, \dots, d_{gK_g}^\diamond]^T$ with $d_{gk}^\diamond = \frac{\lambda_{gk}^\diamond}{\sigma_{gk}^2} \left(1 + \frac{1}{\alpha_g} \right) \mathbf{h}_{gk}^H \mathbf{w}_g^\diamond$, and $\{\lambda_{gk}^\diamond\}$ are corresponding optimal dual variables.

Theorem 1 coincides with the optimal structure discovered in [25]. But the proof is much simpler and more intuitive, since it is built on the LICQ and KKT conditions of the original problem.

By directly setting equation (7) equal to zero, the optimal beamforming structure for problem (5) has another equivalent form, as given in the following Corollary 1.

Corollary 1. The optimal multicast beamforming solution \mathbf{w}_g^\diamond in (10) has the following equivalent form

$$\mathbf{w}_g^\diamond = \left(\mathbf{I}_L + \sum_{i=1, i \neq g}^G \mathbf{H}_i \boldsymbol{\Theta}_i^\diamond \mathbf{H}_i^H \right)^{-1} \mathbf{H}_g \tilde{\mathbf{d}}_g^\diamond, \forall g \in \mathcal{G}, \quad (11)$$

where $\boldsymbol{\Theta}_i^\diamond$ is the same as in (10), and $\tilde{\mathbf{d}}_g^\diamond \triangleq [\tilde{d}_{g1}^\diamond, \dots, \tilde{d}_{gK_g}^\diamond]^T$ with $\tilde{d}_{gk}^\diamond = \frac{\lambda_{gk}^\diamond}{\alpha_g \sigma_{gk}^2} \mathbf{h}_{gk}^H \mathbf{w}_g^\diamond$.

Although the parameters $\boldsymbol{\Theta}_g^\diamond$ and \mathbf{d}_g^\diamond are challenging to obtain due to the NP-hard nature of problem (5), the optimal multicast beamforming structure brings valuable insights to the beamforming design. This is particularly evident when it is used to reduce the dimensions of optimization variables, which we will discuss later.

So far, we have attained the optimal beamforming structure for the power minimization problem (5). However, it remains challenging to solve the general utility problem (4). In the following subsections, we will identify the optimal multicast beamforming structure for problem (4) and discuss some valuable insights. This is a major contribution of this work.

C. Optimal Multi-group Multicast Beamforming Structure for General Utility Function Maximization

In this subsection, we aim to identify the optimal beamforming structure for the generalized utility problem (4) using the SIT duality approach. Introduced in [29], SIT duality is an optimization approach for calculating the global-optimal solution for non-convex optimization problems. It has shown its effectiveness in solving various resource allocation problems, as demonstrated in [31], [32]. To illustrate the SIT principle, we first exchange the objective function and the constraint in (4), resulting in the following SIT dual problem

$$\min_{\mathbf{W}} \text{Tr}(\mathbf{W}\mathbf{W}^H) \quad (12a)$$

$$\text{s.t. } f(R_1, \dots, R_G) \geq f(\beta_1^\diamond, \dots, \beta_G^\diamond), \quad (12b)$$

where $\beta_g^\diamond, \forall g \in \mathcal{G}$ denotes the optimal achievable rate for the multicast stream s_g at the global-optimal solution of the original problem (4). Given the assumption that $f(R_1, \dots, R_G)$ is strictly increasing with respect to $\{R_1, \dots, R_G\}$, problem (12) can be further reformulated as problem (5) where the QoS threshold is given as $\alpha_g^\diamond = \exp(\beta_g^\diamond) - 1$. The SIT principle tells that the optimal solution of (4) can be obtained by solving a

sequence of power minimization problems (5) with increasing SINR constraints α_g° . The optimal α_g° can be obtained by a G -dimensional bisection search.

Based on the principle of SIT, the SIT duality between problem (4) and problem (5) can be established. Specifically, let $\mathbf{H} = [\mathbf{H}_1, \dots, \mathbf{H}_G]$ and $\boldsymbol{\sigma} = [\sigma_{11}, \dots, \sigma_{GK_G}]^T$, a mapping of the general utility problem (4) is defined as

$$\mathcal{U} : \mathbb{R}_+ \rightarrow \mathbb{R}_+^G, \beta^\circ = \mathcal{U}(P_t | \mathbf{H}, \boldsymbol{\sigma}), \quad (13)$$

where $\beta^\circ = [\beta_1^\circ, \dots, \beta_G^\circ]^T$. $\mathcal{U}(P_t | \mathbf{H}, \boldsymbol{\sigma})$ solves problem (4) based on the input parameter P_t , the output corresponds to using the optimal solution \mathbf{W}° to compute the optimal rate vector β° . Also, define the corresponding mapping of the power minimization problem (5) as

$$\mathcal{P} : \mathbb{R}_+^G \rightarrow \mathbb{R}_+, P_t = \mathcal{P}(\beta^\circ | \mathbf{H}, \boldsymbol{\sigma}). \quad (14)$$

Similarly, $\mathcal{P}(\beta^\circ | \mathbf{H}, \boldsymbol{\sigma})$ solves problem (5) based on the input parameters β° , the output corresponds to the minimized transmit power at the optimal solution. Then, the SIT dual relation between problem (4) and problem (5) is described in the following Proposition 1.

Proposition 1. *The SIT duality between problem (4) and problem (5) is established as*

$$\begin{aligned} P_t &= \mathcal{P}(\mathcal{U}(P_t | \mathbf{H}, \boldsymbol{\sigma}) | \mathbf{H}, \boldsymbol{\sigma}) \\ \beta^\circ &= \mathcal{U}(\mathcal{P}(\beta^\circ | \mathbf{H}, \boldsymbol{\sigma}) | \mathbf{H}, \boldsymbol{\sigma}) \end{aligned} \quad (15)$$

Proof: This conclusion can be obtained directly by using the proofs of SIT duality in existing works [29], [31], [32]. Due to space limitations, we omit the proof details in this work. ■

The SIT duality (15) implies that the general utility problem (4) can be solved by searching over rate targets β , such that the optimal objective value of solving (5) for a given rate target β° is equivalent to the constraint upperbound P_t in (4b). Therefore, problems (4) and (5) share the same optimal beamforming structure as shown in Theorem 2.

Theorem 2. *The optimal beamforming solution structures for both problem (4) and problem (5) are equivalent to*

$$\mathbf{W}^\circ = (\mathbf{I}_L + \mathbf{H}\boldsymbol{\Theta}^\circ\mathbf{H}^H)^{-1} \mathbf{H}\mathbf{D}^\circ \quad (16)$$

where $\boldsymbol{\Theta}^\circ = \text{blkdiag}\{\boldsymbol{\Theta}_1^\circ, \dots, \boldsymbol{\Theta}_G^\circ\}$ and $\mathbf{D}^\circ = \text{blkdiag}\{\mathbf{d}_1^\circ, \dots, \mathbf{d}_G^\circ\}$ are some parameters.

Although it remains challenging to determine the optimal achievable rate target β° , the SIT duality helps to identify the optimal beamforming structure for problem (4).

D. Insights from the Optimal Beamforming Structure

To better characterize the optimal multi-group multicast beamforming structure in (16), we further rewrite it as

$$\mathbf{W}^\circ = (\mathbf{I}_L + \mathbf{H}\boldsymbol{\Theta}^\circ\mathbf{H}^H)^{-1} \mathbf{H}\mathbf{B}^\circ\mathbf{P}^\circ, \quad (17)$$

where $\mathbf{B}^\circ \triangleq \text{blkdiag}\{\mathbf{b}_1^\circ, \dots, \mathbf{b}_G^\circ\}$ with $\mathbf{b}_g^\circ \triangleq [b_{g1}^\circ, \dots, b_{gK_G}^\circ]^T$ and $\mathbf{P}^\circ \triangleq \text{diag}\{\sqrt{p_1^\circ}, \dots, \sqrt{p_G^\circ}\}$. In this form, it is evident that the optimal multi-group multicast beamforming structure consists of the following four parts:

- The first part \mathbf{H} is a complete channel matrix, which contains channel directions towards all users. These directions are also known as MRT directions.
- The second part $(\mathbf{I}_L + \mathbf{H}\boldsymbol{\Theta}^\circ\mathbf{H}^H)^{-1}$ is the inversion of the sum of an identity matrix and a weighted channel covariance matrix. It rotates the MRT directions to reduce the inter-group interference. The parameter θ_{gk}° represents the priority assigned to user k in group g , with a larger value indicating that the beamforming vectors of other groups are more orthogonal to the corresponding channel \mathbf{h}_{gk} .
- The third part \mathbf{B}° is a block-diagonalized coefficient matrix, which is the primary difference between multicast and unicast. Parameter b_{gk}° represents the priority of user k in group g , with a larger values indicating that the group beamforming direction \mathbf{w}_g is more aligned to \mathbf{h}_{gk} .
- The fourth part \mathbf{P}° is the power allocation matrix containing the power allocated to all beamforming vectors $\{\mathbf{w}_g\}$.

Considering a special case when there is a single user group g , i.e., single-group multicast transmission, the corresponding optimal beamforming structure in (11) is simplified as $\mathbf{w}_g^\circ = \mathbf{H}_g\mathbf{d}_g^\circ$. This implies that the second part is an identity matrix and the optimal beamforming solution is determined by directly optimizing the weight vector $\mathbf{d}_g \in \mathbb{C}^{K_g \times 1}$ instead of the beamforming vector $\mathbf{w}_g \in \mathbb{C}^{L \times 1}$. Thus, the optimal weight vector \mathbf{d}_g° for maximizing the minimum received signal power $|\mathbf{h}_{gk}^H \mathbf{w}_g|^2$ is given as

$$\mathbf{d}_g^\circ = \arg \max_{\mathbf{d}_g} \min_{k \in \mathcal{K}_g} \{|\mathbf{h}_{gk}^H \mathbf{H}_g \mathbf{d}_g|^2\} \text{ s.t. } \|\mathbf{H}_g \mathbf{d}_g\|^2 \leq P_t. \quad (18)$$

Note that $\mathbf{w}_g^\circ = \mathbf{H}_g\mathbf{d}_g^\circ$ is the optimal beamforming solution when the number of groups is $G = 1$, but it is not optimal for multi-group multicast scenarios since the inter-group interference is not considered.

Regarding multi-group multicast scenarios, the second part $(\mathbf{I}_L + \mathbf{H}\boldsymbol{\Theta}^\circ\mathbf{H}^H)^{-1}$ is required to be considered. This component serves to rotate the group channel matrix \mathbf{H}_g into the null space of $\mathbf{H}_{-g} \triangleq \{\mathbf{h}_{11}, \dots, \mathbf{h}_{g-1, K_{g-1}}, \mathbf{h}_{g+1, K_{g+1}}, \dots, \mathbf{h}_{GK_G}\}$, thereby mitigating inter-group interference. In general, it is hard to determine the optimal $\boldsymbol{\Theta}^\circ$ and \mathbf{D}° due to the NP-hard nature of the multicast beamforming design. In Section IV, we will propose an ultra-low-complexity algorithm based on the optimal multicast beamforming structure to address such issue.

III. LOW-DIMENSIONAL BEAMFORMING STRUCTURE

The primary challenge of finding the optimal beamforming solution to problem (4) lies in the undetermined parameter matrices $\boldsymbol{\Theta}^\circ$ and \mathbf{D}° . Although the optimal parameter matrices $\boldsymbol{\Theta}$ and \mathbf{D} are challenging to calculate, they can be easily attained or even negligible in some asymptotic scenarios, leading to low-complexity and low-dimensional beamforming solutions. In this section, we initially explore two types of low-dimensional structures: one being universal, and the other being asymptotic. We then extend some well-known low-complexity beamforming algorithms to multi-group multicast

scenarios, leveraging the asymptotic analysis of the optimal parameter Θ° . Subsequently, we introduce low-dimensional reformulations for the original problems (4) and (5).

A. Range Space (RS) Beamforming

In XL-MIMO systems where the number of transmit antennas is much larger than the number of total users, i.e., $L \gg K$, the computational complexity of calculating the optimal beamforming sharply increases with L . Here, we provide a low-dimensional structure to reduce the computational complexity by introducing the following Proposition 2.

Proposition 2. *Any optimal solution \mathbf{w}_g° of problem (4) and problem (5) must exist within the range space of the complete channel matrix \mathbf{H} , i.e., $\mathbf{w}_g^\circ = \mathbf{H}\mathbf{a}_g^\circ, \forall g \in \mathcal{G}$, with $\mathbf{a}_g^\circ \in \mathbb{C}^{K \times 1}$.*

Proof: By applying matrix identity $(\mathbf{I}_L + \mathbf{X}\mathbf{Y})^{-1}\mathbf{X} = \mathbf{X}(\mathbf{I}_K + \mathbf{Y}\mathbf{X})^{-1}$ where $\mathbf{X} \in \mathbb{C}^{L \times K}$ and $\mathbf{Y} \in \mathbb{C}^{K \times L}$, any optimal solution shown in (16) can be rewritten as

$$\mathbf{W}^\circ = \mathbf{H}(\mathbf{I}_K + \Theta^\circ \mathbf{H}^H \mathbf{H})^{-1} \mathbf{D}^\circ. \quad (19)$$

Denote $\mathbf{A}^\circ \triangleq (\mathbf{I}_K + \Theta^\circ \mathbf{H}^H \mathbf{H})^{-1} \mathbf{D}^\circ \in \mathbb{C}^{K \times G}$, we conclude that any optimal beamforming vector for each user group g must lie in the RS of the complete channel matrix. ■

Leveraging Proposition 2, the RS beamforming is given as

$$\mathbf{W} = \mathbf{H}\mathbf{A}, \quad (20)$$

where $\mathbf{A} \in \mathbb{C}^{K \times G}$ has a lower dimension compared to \mathbf{W} . Notably, the dimension of \mathbf{A} is independent of the number of transmit antennas L . It implies that substituting \mathbf{W} with $\mathbf{H}\mathbf{A}$ in problem (4) and (5) significantly reduces the optimization dimension of the beamforming matrix. Further elaboration will be provided in Section III-F.

In the following subsections, we discover more low-dimensional beamforming structures based on the asymptotic analysis of the optimal parameter Θ° in (19).

B. MRT Beamforming

In the low SNR regime, i.e., $\sigma_{gk}^2 \rightarrow \infty$ (therefore $\theta_{gk} = \frac{\lambda_{gk}}{\sigma_{gk}^2} \rightarrow 0$), the system is noise-limited and the beamforming matrix in (19) converges to

$$\lim_{P_t \rightarrow 0} \mathbf{W}^\circ = \mathbf{H}\mathbf{D}^\circ, \quad (21)$$

where the inversion part converges to the identity matrix and \mathbf{D}° includes both the asymptotic power allocation and coefficients of the linear combination for the group-channel direction. It implies that MRT beamforming achieves a good performance in the low SNR regime. Thus, a natural extension of the well-known MRT beamforming in multi-group multicast transmission is given as

$$\mathbf{W} = \mathbf{H}\mathbf{D}, \quad (22)$$

where $\mathbf{D} \triangleq \text{blkdiag}\{\mathbf{d}_1, \dots, \mathbf{d}_G\} \in \mathbb{C}^{K \times G}$ with $\mathbf{d}_g \triangleq [d_{g1}, \dots, d_{gK}]^T$. It differs from Proposition 2 since \mathbf{D} is a block diagonal matrix containing K variables while \mathbf{A} is a full matrix containing $K \times G$ variables. This strategy maximizes the minimum received signal power $|\mathbf{h}_{gk}^H \mathbf{w}_g|^2$ received at group g while ignoring the interference from other user groups.

C. ZF-based and Regularized ZF-based Beamforming

When SNR is high, i.e., $P_t \rightarrow \infty$, the system is in the interference-limited region. We focus on the case $L \geq K$ with at least one spatial degree-of-freedom per user. In this scenario, each parameter θ_{gk} tends to infinity and (19) converges to

$$\lim_{P_t \rightarrow \infty} \mathbf{W}^\circ = \mathbf{H}(\mathbf{H}^H \mathbf{H})^{-1} \Theta^{\circ-1} \mathbf{D}^\circ. \quad (23)$$

The extension of ZF beamforming in multi-group multicast transmission is

$$\mathbf{W} = \mathbf{H}(\mathbf{H}^H \mathbf{H})^{-1} \mathbf{D}. \quad (24)$$

Similar to the unicast-only transmission, to achieve numerical stability and robustness to channel uncertainty, regularized ZF (RZF) beamforming is usually considered by forcing $\sum_{g=1}^G \sum_{k=1}^{K_g} \theta_{gk} = P_t$ [33]. This leads to the following RZF beamforming

$$\mathbf{W} = \mathbf{H} \left(\frac{1}{P_t} \mathbf{I}_K + \mathbf{H}^H \mathbf{H} \right)^{-1} \mathbf{D}. \quad (25)$$

D. Multicast ZF and RZF-based Beamforming

Recall that the optimal multi-group multicast beamforming has an equivalent form (11), from which we obtain

$$\lim_{P_t \rightarrow \infty} \mathbf{w}_g^\circ = (\mathbf{H}_{-g} \mathbf{H}_{-g}^H)^\dagger \mathbf{H}_g \tilde{\mathbf{d}}_g^\circ, \forall g \in \mathcal{G} \quad (26)$$

where \dagger denotes the pseudo-inverse of a matrix. From this asymptotic result, we propose the following two useful low-dimensional beamforming structures

$$\mathbf{w}_g = (\mathbf{H}_{-g} \mathbf{H}_{-g}^H)^\dagger \mathbf{H}_g \mathbf{d}_g, \forall g \in \mathcal{G}, \quad (27a)$$

$$\mathbf{w}_g = \left(\frac{1}{P_t} \mathbf{I}_L + \mathbf{H}_{-g} \mathbf{H}_{-g}^H \right)^\dagger \mathbf{H}_g \mathbf{d}_g, \forall g \in \mathcal{G}, \quad (27b)$$

which are referred as multicast ZF (MZF) and multicast RZF (MRZF), respectively.

Remark 2. *Although (27a) has a similar structure with (24), they have different mathematical implications. As $P_t \rightarrow \infty$, the matrix $(\mathbf{H}_{-g} \mathbf{H}_{-g}^H)^\dagger$ rotates group channel matrix \mathbf{H}_g into the null space of the matrix \mathbf{H}_{-g} , which implies any group-channel matrix \mathbf{H}_g satisfies $\mathbf{H}_g^H (\mathbf{H}_{-i} \mathbf{H}_{-i}^H)^\dagger \mathbf{H}_i = \mathbf{0}, \forall i \neq g, i \in \mathcal{G}$. Note that $\mathbf{H}^H \left[(\mathbf{H}_{-1} \mathbf{H}_{-1}^H)^\dagger \mathbf{H}_1, \dots, (\mathbf{H}_{-G} \mathbf{H}_{-G}^H)^\dagger \mathbf{H}_G \right]$ is a block diagonal matrix and therefore the MZF beamforming (27a) is sufficient to eliminate the inter-group interference. This contrasts to the matrix inversion $(\mathbf{H}^H \mathbf{H})^{-1}$ in the classical ZF beamforming (24), which rotates all channel vectors to be orthogonal to each other, i.e., $\mathbf{H}^H \mathbf{H} (\mathbf{H}^H \mathbf{H})^{-1}$ results in a diagonal matrix.*

E. Large-scale MIMO Systems

Next, we delve into the asymptotic beamforming structure for XL-MIMO when the number of transmit antenna L goes to infinite. In (19), the value of $\mathbf{H}^H \mathbf{H}$ grows with L , it is obviously that

$$\lim_{L \rightarrow \infty} \mathbf{W}^\circ = \mathbf{H}(\mathbf{H}^H \mathbf{H})^{-1} \Theta^{\circ-1} \mathbf{D}^\circ, \quad (28)$$

which implies that the ZF-based beamforming is asymptotically optimal when L goes to infinity.

A similar low dimensional structure has been proposed in [25] and adopted by [20], [25], [27], [28]. This approach employs an asymptotic fixed-point iteration to directly calculate the rotated channel matrix $\mathbf{H} = \mathbf{H}(\mathbf{I}_K + \Theta \mathbf{H}^H \mathbf{H})^{-1}$ and then optimize \mathbf{D} . It should be noted that the proposed approach in [25] is only asymptotically optimal when $L \rightarrow \infty$. But it is tailored for the QoS problem and cannot be extended to solve the general utility problem (4).

F. Low-dimensional Reformulations

The low-dimensional structures introduced in the previous subsections are advantageous for reducing the computational complexity in beamforming design by removing the dependence of the beamforming dimension on the number of transmit antenna L . Here, we take the RS structure (20) as an example to show its benefits. To be specific, by replacing the original high-dimensional beamforming matrix, i.e., $\mathbf{W} \in \mathbb{C}^{L \times G}$, with the low-dimensional RS beamforming matrix i.e., $\mathbf{H}\mathbf{A}$, the original problem (4) and (5) can be respectively reformulated as

$$\max_{\mathbf{A}} f(R_1, \dots, R_G) \quad (29a)$$

$$\text{s.t. } \text{Tr}(\mathbf{A}\mathbf{A}^H \mathbf{F}) \leq P_t, \quad (29b)$$

where

$$R_g = \min_{k \in \mathcal{K}_g} \log \left(1 + \frac{|\mathbf{f}_{gk}^H \mathbf{a}_g|^2}{\sum_{i=1, i \neq g}^G |\mathbf{f}_{gk}^H \mathbf{a}_i|^2 + \sigma_{gk}^2} \right), \quad (30)$$

and

$$\min_{\mathbf{A}} \text{Tr}(\mathbf{A}\mathbf{A}^H \mathbf{F}) \quad (31a)$$

$$\text{s.t. } \frac{|\mathbf{f}_{gk}^H \mathbf{a}_g|^2}{\sum_{i=1, i \neq g}^G |\mathbf{f}_{gk}^H \mathbf{a}_i|^2 + \sigma_{gk}^2} \geq \alpha_g, \forall k \in \mathcal{K}_g, \forall g \in \mathcal{G}, \quad (31b)$$

where $\mathbf{F} \triangleq [\mathbf{f}_{11}, \dots, \mathbf{f}_{GK_G}] \in \mathbb{C}^{K \times K}$ with $\mathbf{f}_{gk} = \mathbf{H}^H \mathbf{h}_{gk}$ and $\mathbf{A} \triangleq [\mathbf{a}_1, \dots, \mathbf{a}_G] \in \mathbb{C}^{K \times G}$. For both reformulated problems, the dimension of the optimization variables decreases from $L \times G$ to $K \times G$ and the complexity of matrix inversion decreases from $\mathcal{O}(L^3)$ to $\mathcal{O}(K^3)$.

IV. EFFICIENT BEAMFORMING ALGORITHMS FOR WSR MAXIMIZATION

In this section, we take WSR as an instance of the general utility function, i.e., $f(R_1, \dots, R_G) = \sum_{g=1}^G \zeta_g R_g$, where ζ_g refers to the weight of user group g . Our focus is on deriving efficient beamforming algorithms to solve the following WSR maximization problem:

$$\max_{\mathbf{W}} \sum_{g=1}^G \zeta_g R_g, \text{ s.t. } \text{Tr}(\mathbf{W}\mathbf{W}^H) \leq P_t. \quad (32)$$

where $R_g = \min_{k \in \mathcal{K}_g} \{\log(1 + \gamma_{gk})\}$. This problem is more difficult to solve than the MMF problem when $f(R_1, \dots, R_G) = \min_{g \in \mathcal{G}} R_g$, since the optimal rate targets

varies across distinct user groups. Utilizing SIT duality requires a G -dimensional exhaustive search over the optimal rate targets, leading to exponential computational complexity, making it impractical to solve such problem. Generally, problem (32) has two primary challenges:

- 1) Non-convex SINR expressions for all users;
- 2) Non-smooth rate expressions for all multicast streams.

The first challenge has been extensively studied in unicast-only transmission, classical algorithms such as WMMSE, FP, and WSR-MM have emerged to address the non-convexity of SINR expressions. The second challenge posed by non-smooth max-min rate expressions has led to the introduction of some approaches, i.e., linearization [34], subgradient ascent (SA) algorithm [35], and the LogSumExp (LSE)-based algorithm [36]. These approaches are briefly introduced below:

- Linearization involves introducing auxiliary variables to substitute the max-min rates in the objective function and adding additional rate constraints for all user groups to reformulate the problem [34]. Such approach inevitably increases the optimization dimension.
- The SA algorithm [35] is a typical approach for solving non-smooth problems. Based on a certain step size, it iteratively updates the solution towards the subgradient direction of the non-smooth objective function until convergence. However, choosing an appropriate rule to update the step size is challenging and can significantly impact the convergence speed.
- The LSE method approximates the non-smooth objective function using the LSE function [36]. For example, the LSE of R_g is $\text{LSE}_g = -\mu \log \left(\sum_{k=1}^{K_g} \exp(-R_{gk}/\mu) \right)$, where $R_{gk} = \log(1 + \gamma_{gk})$. However, choosing a proper value for μ is challenging. The complicated LSE function introduces extra challenges in solving the original problem, and the approximation error prohibits the identification of the optimal beamforming structure.

Due to the aforementioned limitations of existing algorithms, we next propose a novel optimization algorithm to solve the non-convex non-smooth WSR problem (32) based on the optimal and low-complexity beamforming structures we introduced in Section II and Section III.

A. Problem Reformulation

To better characterize the multi-group multicast beamforming, we move the power constraint into the SINR expression leading to the following unconstrained problem:

$$\max_{\mathbf{W}} \sum_{g=1}^G \zeta_g \min_{k \in \mathcal{K}_g} \{\log(1 + \hat{\gamma}_{gk})\}, \quad (33)$$

where

$$\hat{\gamma}_{gk} \triangleq \frac{|\mathbf{h}_{gk}^H \mathbf{w}_g|^2}{\sum_{i \neq g} |\mathbf{h}_{gk}^H \mathbf{w}_i|^2 + \frac{\sigma_{gk}^2}{P_t} \text{Tr}(\mathbf{W}\mathbf{W}^H)}. \quad (34)$$

The relation between (32) and (33) is provided in the following Proposition 3.

Proposition 3. For any locally optimal solution \mathbf{W}^\diamond of problem (32), there exists a corresponding locally optimal solution \mathbf{W}^\ddagger of the unconstrained problem (33) such that $\mathbf{W}^\diamond = \sqrt{\frac{P_t}{\text{Tr}(\mathbf{W}^\ddagger \mathbf{W}^\ddagger H)}} \mathbf{W}^\ddagger$.

Proof: The detail proof follows the procedure in [37]. ■

Leveraging Proposition 3, we can efficiently solve problem (32) by directing our focus towards solving the unconstrained problem (33) in the following.

B. Cyclic Maximization Method

In this subsection, we introduce a cyclic maximization (CM)-based method to solve problem (33). The main idea of CM is to construct a high dimensional surrogate objective function and then solve each block cyclically to obtain a stationary point of the original non-convex problem [38], [39].

We start with introducing the following Proposition 4 to transform (33) into a more tractable form.

Proposition 4. By introducing auxiliary variables $\{\xi_{gk}, \eta_{gk}\}$, problem (33) can be equivalently reformulated as

$$\max_{\mathbf{W}, \xi, \eta} \sum_{g=1}^G \zeta_g \min_{k \in \mathcal{K}_g} \{h_{gk}(\mathbf{W}, \xi_{gk}, \eta_{gk})\}, \quad (35)$$

where $\xi \triangleq [\xi_{11}, \dots, \xi_{GK_G}]^T$, $\eta \triangleq [\eta_{11}, \dots, \eta_{GK_G}]^T$, and

$$h_{gk}(\mathbf{W}, \xi_{gk}, \eta_{gk}) \triangleq \log(1 + \xi_{gk}) + 2\sqrt{1 + \xi_{gk}} \Re\{\eta_{gk}^H \mathbf{h}_{gk}^H \mathbf{w}_g\} - |\eta_{gk}|^2 \left(\sum_{i=1}^G |\mathbf{h}_{gk}^H \mathbf{w}_i|^2 + \frac{\sigma_{gk}^2}{P_t} \text{Tr}(\mathbf{W} \mathbf{W}^H) \right) - \xi_{gk}. \quad (36)$$

Proof: The convex function $\log(\frac{1}{x})$ with $x \in \mathbb{R}_+$ has the following lower bound

$$\log\left(\frac{1}{x}\right) \geq \log\left(\frac{1}{x_0}\right) - \frac{1}{x_0}(x - x_0) \quad (37)$$

with equality achieved at $x_0 = x$. By plugging $x = \frac{1}{1 + \hat{\gamma}_{gk}}$ and $x_0 = \frac{1}{1 + \xi_{gk}}$ into (37), we obtain the following surrogate function

$$\begin{aligned} \log(1 + \hat{\gamma}_{gk}) &\geq \log(1 + \xi_{gk}) - \frac{1 + \xi_{gk}}{1 + \hat{\gamma}_{gk}} + 1 \\ &\geq \log(1 + \xi_{gk}) - \xi_{gk} + \frac{(1 + \xi_{gk}) |\mathbf{h}_{gk}^H \mathbf{w}_g|^2}{\sum_{i=1}^G |\mathbf{h}_{gk}^H \mathbf{w}_i|^2 + \frac{\sigma_{gk}^2}{P_t} \text{Tr}(\mathbf{W} \mathbf{W}^H)} \end{aligned}$$

with equality holding when $\xi_{gk} = \hat{\gamma}_{gk}$. Further, the convex fractional function $\frac{|x|^2}{y}$ with $x \in \mathbb{C}$ and $y \in \mathbb{R}_+$ can be lower bounded by its first order Taylor expansion as

$$\frac{|x|^2}{y} \geq 2\Re\left\{\frac{x_0^H}{y_0} x\right\} - \frac{|x_0|^2}{y_0^2} y \quad (38)$$

with equality achieved at $(x_0, y_0) = (x, y)$. By substituting $x = \sqrt{1 + \xi_{gk}} \mathbf{h}_{gk}^H \mathbf{w}_g$, $y = \sum_{i=1}^G |\mathbf{h}_{gk}^H \mathbf{w}_i|^2 + \frac{\sigma_{gk}^2}{P_t} \text{Tr}(\mathbf{W} \mathbf{W}^H)$ and $\eta_{gk} = x_0/y_0$ into (38), we obtain the two-layer surrogate function $h_{gk}(\mathbf{W}, \xi_{gk}, \eta_{gk})$ in (36). ■

Problem (35) remains non-convex, but it is obvious that, it can be solved by the CM method with the following updates

Algorithm 1: Standard CM framework for problem (32)

- 1 **Initilize:** Set initial feasible $\mathbf{W}^{[0]}$; set $t = 1$;
 - 2 **repeat**
 - 3 $t \leftarrow t + 1$;
 - 4 Update the auxiliary variables $\xi_{gk}^{[t]}$ and $\eta_{gk}^{[t]}$ by (39a) and (39b) for $k \in \mathcal{K}_g, \forall g \in \mathcal{G}$;
 - 5 Update $\mathbf{W}^{[t]}$ by solving problem (40) optimally;
 - 6 **until** convergence;
 - 7 Scale and output $\mathbf{W}^\diamond = \sqrt{\frac{P_t}{\text{Tr}(\mathbf{W}^{[t]} \mathbf{W}^{[t]H})}} \mathbf{W}^{[t]}$.
-

$$\xi_{gk}^{[t+1]} = \gamma_{gk}^{[t]}, \quad (39a)$$

$$\eta_{gk}^{[t+1]} = \frac{\sqrt{1 + \xi_{gk}^{[t+1]}} \mathbf{h}_{gk}^H \mathbf{w}_g^{[t]}}{\sum_{i=1}^G |\mathbf{h}_{gk}^H \mathbf{w}_i^{[t]}|^2 + \frac{\sigma_{gk}^2}{P_t} \text{Tr}(\mathbf{W}^{[t]} \mathbf{W}^{[t]H})}, \quad (39b)$$

$$\mathbf{W}^{[t+1]} = \arg \max_{\mathbf{W}} \sum_{g=1}^G \zeta_g \min_{k \in \mathcal{K}_g} \left\{ h_{gk}(\mathbf{W}, \xi_{gk}^{[t+1]}, \eta_{gk}^{[t+1]}) \right\}. \quad (39c)$$

For given $\{\xi, \eta\}$, the subproblem (39c) with respect to \mathbf{W} is a non-smooth convex quadratic programming and thus can be directly solved using standard convex optimization approaches (i.e., interior-point methods) implemented by a certain solver (i.e., SeDuMi) in the CVX toolbox [18]. Such approach of using CM to solve problem (35) as well as using the standard solvers in CVX to solve problem (40) is referred as the standard CM method as summarized in Algorithm 1.

The equivalence between the CM framework and the classical MM theory has been confirmed in [39]. Besides, the recent study [17] has established the equivalence between WMMSE, FP, and MM for solving the WSR problems. Therefore, we could infer that algorithms using convex approximation and employing a standard optimization solver in CVX [18] to solve each convex subproblem exhibit comparable performance.

C. Proposed Efficient Optimization Algorithms

Although the standard CM algorithm in Algorithm 1 successfully solves subproblem (39c) using the standard CVX toolbox, this approach is not cost-effective due to the substantial time occupied to parse and canonicalize the original subproblem into a standard form for CVX solvers to understand. Moreover, problem (39c) is non-differentiable at the points where two or more functions of $\{h_{gk}\}$ share the same value. To avoid these limitations of solving (39c) directly using CVX, we propose a novel optimization algorithm based on its optimal beamforming structure. Specifically, by introducing a set of slack auxiliary variables $\mathbf{z} = [z_1, \dots, z_G]^T$, we aim to solve the following equivalent problem of (39c):

$$\max_{\mathbf{W}, \mathbf{z}} \sum_{g=1}^G \zeta_g z_g \quad (40a)$$

$$\text{s.t. } z_g \leq h_{gk}(\mathbf{W}, \xi_{gk}, \eta_{gk}), \forall g \in \mathcal{G}, \forall k \in \mathcal{K}_g. \quad (40b)$$

Problem (40) is a smooth convex SOCP problem and can be efficiently solved via its Lagrange dual problem. The Lagrangian function of (40) is given as

$$\mathcal{L}_{(40)}(\boldsymbol{\delta}, \mathbf{W}, \mathbf{z}) \triangleq \sum_{g=1}^G \zeta_g z_g - \sum_{g=1}^G \sum_{k=1}^{K_g} \delta_{gk} (z_g - h_{gk}(\mathbf{W}, \xi_{gk}, \eta_{gk})),$$

where $\delta_{gk} \geq 0$ is the dual variable corresponding to constraint (40b), and $\boldsymbol{\delta} \triangleq [\boldsymbol{\delta}_1, \dots, \boldsymbol{\delta}_G]$ with $\boldsymbol{\delta}_g \triangleq [\delta_{g1}, \dots, \delta_{gK_g}]^T$. The first-order derivatives of the Lagrange function $\mathcal{L}_{(40)}(\boldsymbol{\delta}, \mathbf{W}, \mathbf{z})$ with respect to z_g and \mathbf{w}_g are respectively given as

$$\frac{\partial \mathcal{L}_{(40)}}{\partial z_g} = \zeta_g - \sum_{k=1}^{K_g} \delta_{gk},$$

$$\frac{\partial \mathcal{L}_{(40)}}{\partial \mathbf{w}_g} = \sum_{k=1}^{K_g} 2\hat{d}_{gk} \mathbf{h}_{gk} - \sum_{i=1}^G \sum_{k=1}^{K_i} 2 \left(\hat{\theta}_{ik} \mathbf{h}_{ik} \mathbf{h}_{ik}^H + \frac{\delta_{ik} \sigma_{ik}^2}{P_t} \mathbf{I}_L \right) \mathbf{w}_g,$$

where $\hat{d}_{gk}, \forall g \in \mathcal{G}, k \in \mathcal{K}_g$, and $\hat{\theta}_{ik}, \forall i \in \mathcal{G}, k \in \mathcal{K}_i$ are respectively defined as

$$\hat{d}_{gk} \triangleq \delta_{gk} \eta_{gk} \sqrt{1 + \xi_{gk}}, \quad \hat{\theta}_{ik} \triangleq \delta_{ik} |\eta_{ik}|^2. \quad (41)$$

Since (40) is convex and strictly feasible, it satisfies the Slater's condition and the strong duality holds [40]. Therefore, the optimal solution of (40), together with the optimal Lagrange dual variable, satisfies the following KKT conditions

$$\zeta_g - \sum_{k=1}^{K_g} \delta_{gk} = 0, \quad g \in \mathcal{G}, \quad (42a)$$

$$\sum_{k=1}^{K_g} 2\hat{d}_{gk} \mathbf{h}_{gk} - \sum_{i=1}^G \sum_{k=1}^{K_i} 2 \left(\hat{\theta}_{ik} \mathbf{h}_{ik} \mathbf{h}_{ik}^H + \frac{\delta_{ik} \sigma_{ik}^2}{P_t} \mathbf{I}_L \right) \mathbf{w}_g = \mathbf{0}, \quad g \in \mathcal{G}, \quad (42b)$$

$$\delta_{gk} (z_g - h_{gk}) = 0, \quad g \in \mathcal{G}, k \in \mathcal{K}_g, \quad (42c)$$

where (42a) and (42b) are the first-order stationary conditions, and (42c) refers to the complementary slackness conditions. The primal and dual feasibility conditions are omitted here.

According to (40), we could directly obtain the optimal slackness variable z_g as $z_g^* = \min_{k \in \mathcal{K}_g} \{h_{gk}\}, \forall g \in \mathcal{G}$. Moreover, from (42b), we further reveal the optimal beamforming structure for problem (40) in Theorem 3.

Theorem 3. *The optimal beamforming solution for problem (40) is given by*

$$\mathbf{w}_g^* = \left(\mathbf{H} \boldsymbol{\Theta}^* \mathbf{H}^H + S_\sigma \mathbf{I} \right)^{-1} \mathbf{H}_g \hat{\mathbf{d}}_g^*, \quad \forall g \in \mathcal{G}, \quad (43)$$

where $\{\delta_{gk}^*\}$ are the optimal dual variables for problem (40), $\boldsymbol{\Theta}^* \triangleq \text{blkdiag}\{\boldsymbol{\Theta}_1^*, \dots, \boldsymbol{\Theta}_G^*\}$ with $\boldsymbol{\Theta}_g^* = \text{diag}\{\hat{\theta}_{g1}^*, \dots, \hat{\theta}_{gK_g}^*\}$ with $\hat{\theta}_{gk}^* = \delta_{gk}^* |\eta_{gk}|^2$, $S_\sigma \triangleq \sum_{i=1}^G \sum_{k=1}^{K_i} \frac{\delta_{ik}^* \sigma_{ik}^2}{P_t}$, and $\hat{\mathbf{d}}_g^* = [\hat{d}_{g1}^*, \dots, \hat{d}_{gK_g}^*]^T$ with $\hat{d}_{gk}^* = \delta_{gk}^* \eta_{gk} \sqrt{1 + \xi_{gk}}$.

It is clear that the beamforming structure (43) shares the same structure with the optimal multi-group multicast beamforming structure (16). Substituting (43) and (42a) into $\mathcal{L}_{(40)}(\boldsymbol{\delta}, \mathbf{W}, \mathbf{z})$, the Lagrange dual problem of (40) is given by

$$\min_{\boldsymbol{\delta} \in \mathcal{H}} \sum_{g=1}^G \sum_{k=1}^{K_g} \delta_{gk} h_{gk}(\mathbf{W}^*, \xi_{gk}, \eta_{gk}), \quad (44)$$

where $\mathcal{H} \triangleq \mathcal{H}_1 \times \dots \times \mathcal{H}_G$ with $\mathcal{H}_g \triangleq \{\delta_{gk} \geq 0 : \sum_{k=1}^{K_g} \delta_{gk} = \zeta_g\}$ and $\mathbf{W}^* \triangleq [\mathbf{w}_1^*, \dots, \mathbf{w}_G^*]$. The dual problem is convex

Algorithm 2: PAGD algorithm for solving problem (40)

- 1 **Initilize:** Set initial feasible $\boldsymbol{\delta}^{[0]} \in \mathcal{H}$, set $j = 1$;
 - 2 **repeat**
 - 3 $j \leftarrow j + 1$;
 - 4 Update the primal variable $\mathbf{w}_g^{[j]}$ by (43) for $\forall g \in \mathcal{G}$;
 - 5 Update the dual variable $\boldsymbol{\delta}_g^{[j]}$ by (45) for $\forall g \in \mathcal{G}$;
 - 6 **until convergence**;
-

and the feasible space $\boldsymbol{\delta} \in \mathcal{H}$ implies that each dual vector $\boldsymbol{\delta}_g$ lies in the hyperplane \mathcal{H}_g . This motivates us to solve problem (44) base on the projected adaptive gradient descent (PAGD) algorithm.

PAGD is an optimization algorithm that minimize a function iteratively by updating the solution towards the opposite direction of the gradient with an adaptive step size in each iterative. It then includes a projection step to project the updated solution onto the feasible set. In this work, we propose to solve problem (44) based on the following updating procedure in each iteration $[j]$:

$$\bar{\delta}_{gk}^{[j+1]} = \delta_{gk}^{[j]} - \tau_{gk}^{[j]} \left(h_{gk}^{[j]} - \min_{i \in \mathcal{K}_g} \{h_{gi}^{[j]}\} \right), \quad g \in \mathcal{G}, k \in \mathcal{K}_g, \quad (45a)$$

$$\boldsymbol{\delta}_g^{[j+1]} = \Pi_{\mathcal{H}_g}(\bar{\boldsymbol{\delta}}_g^{[j+1]}), \quad \forall g \in \mathcal{G}, \quad (45b)$$

where $\bar{\boldsymbol{\delta}}_g \triangleq [\bar{\delta}_{g1}, \dots, \bar{\delta}_{gK_g}]^T$ refers to the intermediate updates before projection, and $\tau_{gk}^{[j]}$ is the step size, given by

$$\tau_{gk}^{[j]} = \frac{\delta_{gk}^{[j]}}{h_{gk}^{[j]} - \min_{i \in \mathcal{K}_g} \{h_{gi}^{[j]}\} + \rho_t^{[j]}}, \quad (46)$$

with an increasing constant number $\rho_t^{[j]} = \rho_c + \rho_v \cdot j$. $\Pi_{\mathcal{H}_g}(\bar{\boldsymbol{\delta}}_g^{[j+1]})$ denotes the projection of $\bar{\boldsymbol{\delta}}_g^{[j+1]}$ onto the hyperplane \mathcal{H}_g , which is defined as

$$\Pi_{\mathcal{H}_g}(\bar{\boldsymbol{\delta}}_g^{[j+1]}) = \bar{\boldsymbol{\delta}}_g^{[j+1]} - \frac{\sum_{k=1}^{K_g} \bar{\delta}_{gk}^{[j+1]} - \zeta_g}{K_g}. \quad (47)$$

The optimal dual vector $\boldsymbol{\delta}^*$ for each convex problem (40) can be obtained using the proposed PAGD algorithm summarized in Algorithm 2. Therefore, the subproblem (39c) is optimally solved by substituting $\boldsymbol{\delta}^*$ into the optimal beamforming solution (43). By employing the CM framework and PAGD to address (32), we establish a highly efficient algorithm referred to as CM-PAGD. In contrast to the standard CM approach, our proposed algorithm exhibits lower computational complexity and ensures no loss in performance. This will be further demonstrated in the simulation section.

Remark 3. *The step size follows the rule of square summable but not summable [35], which typically follows*

$$\tau_{gk}^{[j]} = \frac{x}{y + \rho_v \cdot j}, \quad (48)$$

where $x > 0, y \geq 0$ are problem-specific parameters and ρ_v is a decreasing factor. To ensure $\bar{\delta}_{gk}^{[j+1]} \geq 0$, we have

$$\tau_{gk}^{[j]} \leq \frac{\delta_{gk}^{[j]}}{h_{gk}^{[j]} - \min_{i \in \mathcal{K}_g} \{h_{gi}^{[j]}\}}. \quad (49)$$

Let x and y in (48) be defined as $x = \delta_{gk}^{[j]}$ and $y = h_{gk}^{[j]} - \min_{i \in \mathcal{K}_g} \{h_{gi}^{[j]}\} + \rho_c$, we end up with the proposed step size (46). This step size enables the dual vector $\bar{\delta}_g^{[j+1]}$ within the subspace $\{\delta_{gk} \geq 0 : \sum_{k=1}^{K_g} \delta_{gk} \leq \zeta_g\}$, and it is therefore easy to project it back onto the hyperplane \mathcal{H}_g based on the defined projection rule (47).

D. Low-dimensional Reformulations for Large Scale Systems

As mentioned in Section III, the proposed low-dimensional beamforming structures can be used to reduce the computational complexity of the beamforming design. Here, we take the RS structure $\mathbf{W} = \mathbf{H}\mathbf{A}$ as an example to show its benefits in solving the WSR problem for XL-MIMO systems. By substituting $\mathbf{W} = \mathbf{H}\mathbf{A}$ into (32), the WSR problem is reformulated as

$$\max_{\mathbf{A}} \sum_{g=1}^G \zeta_g \min_{k \in \mathcal{K}_g} \left\{ \log \left(1 + \frac{|\mathbf{f}_{gk}^H \mathbf{a}_g|^2}{\sum_{i=1, i \neq g}^G |\mathbf{f}_{gk}^H \mathbf{a}_i|^2 + \sigma_{gk}^2} \right) \right\} \quad (50a)$$

$$\text{s.t. } \text{Tr}(\mathbf{A}\mathbf{A}^H \mathbf{F}) \leq P_t. \quad (50b)$$

This formulation is equivalent to (32), but with significantly reduced dimensionality in the optimization variables. Therefore, we can solve it using the proposed CM-PAGD methods.

Other low-dimensional reformulations based on MRT, ZF, RZF, MZF, or MRZF follow a similar process as (50). To avoid redundancy, we omit the details of these reformulation here. A comprehensive comparison among different approaches will be provided in the following simulation section.

E. Convergence and Computational Complexity Analysis

1) *Convergence Analysis*: The proposed CM-PAGD algorithm consists of two iteration layers. The outer-layer CM framework outlined in Algorithm 1 is guaranteed to generate a monotonically increasing sequence of objective values for (32), as proven in [15], [16], [39]. Regarding the convergence of the inner-layer iteration for computing the optimal dual variables in Algorithm 2, it is established in [35] that the algorithm is guaranteed to converge if the objective function satisfies the Lipschitz condition. This condition is clearly met in our algorithm since the objective function is continuous differentiable over the convex set \mathcal{H} . For further details, readers can refer to [35].

2) *Computational Complexity Analysis*: The computational complexity of the proposed CM-PAGD algorithm for each iteration is dominated by updating the beamforming matrix (i.e., line 5 of Algorithm 1) based on Algorithm 2. The complexity of Algorithm 2 is dominated by the matrix inversion in line 4, with an order of $\mathcal{O}(GL^3)$. The overall complexity order is $\mathcal{O}(GL^3 \log(\epsilon_1^{-1}) \log(\epsilon_2^{-1}))$, where ϵ_1 refers to the convergence tolerance of the outer-layer CM framework, and ϵ_2 refers to the convergence tolerance of the inner-layer PAGD algorithm.

V. SIMULATION RESULTS

In this section, we evaluate the computational complexity, convergence, and the WSR performance of the proposed CM-PAGD algorithm based on the optimal beamforming structure or other low-dimensional beamforming structures.

A. Simulation Setup

We consider a symmetric multi-group multicast communication network, where $K_g = K_G, \forall g \in \mathcal{G}$. Unless specified otherwise, the default user set consists of $G = 3$ groups, with $K_G = 4$ users per group. The channel of user k is generated i.i.d. as $\mathbf{h}_{gk} \sim \mathcal{CN}(\mathbf{0}, \mathbf{I}_L)$ and the noise variance at user k is set to $\sigma_{gk}^2 = 1$ so that the transmit SNR defined as $\text{SNR} \triangleq P_t / \sigma_{gk}^2$ is numerically equal to the transmit power. For the proposed algorithms, we set the stopping tolerance for both the outer-layer CM framework and inner-layer iterative algorithms as $\epsilon_1 = \epsilon_2 = 10^{-4}$. Additional, the constant $\rho_t^{[j]}$ in (46) is set to $\rho_t^{[j]} = 1 + 0.02 \times j$ for controlling the convergence accuracy of the inner-layer PAGD algorithm. Without loss of generality, we set the weights $\zeta_1 = \zeta_2 = \dots = \zeta_G = 1$ in our simulations. The initialization of the beamforming vectors for the CM framework is based on MRT directions, e.g., $\mathbf{w}_g^{[0]} = \sum_{k=1}^{K_g} \mathbf{h}_{gk}, \forall g \in \mathcal{G}$. All simulation results are averaged over 100 random channel realizations.

B. Baseline Algorithms

All schemes considered in the simulation are summarized as follows:

- **standard CM**: This is the standard CM framework we introduced in Algorithm 1. Each subproblem (39c) is solved using CVX toolbox, leading to an overall computational complexity of $\mathcal{O}([GL]^{3.5} \log(\epsilon_1^{-1}))$.
- **CM-SA**: This refers to the algorithm of employing the CM framework to solve problem (35), while using the SA algorithm [35] to solve each non-smooth surrogate problem directly. The gradient of worst-case user per group is selected as the subgradient [27]. The overall computational complexity is $\mathcal{O}(GL^2 \log(\epsilon_1^{-1}) \log(\epsilon_2^{-2}))$.
- **CM-LSE**: This refers to the algorithm of employing the CM framework to solve problem (35), while using the LSE algorithm [36] to approximate the non-smooth objective function for each surrogate problem [15]. The approximated convex and smooth problem is then solved by the gradient ascent approach. The corresponding computational complexity is $\mathcal{O}(GL^2 \log(\epsilon_1^{-1}) \log(\epsilon_2^{-1}))$.
- **CM-PAGD**: This is the algorithm we proposed based on Algorithm 1 and Algorithm 2. Specifically, for each subproblem (39c) in Algorithm 1, instead of using CVX to solve it directly, we propose to use the PAGD algorithm in Algorithm 2 to address it. CM-PAGD is therefore an optimization toolbox-free algorithm, which reduces the computational complexity. The corresponding computational complexity is $\mathcal{O}(GL^3 \log(\epsilon_1^{-1}) \log(\epsilon_2^{-1}))$.
- **RS CM-PAGD**: This is the algorithm we proposed based on the RS property discovered in (19) and CM-PAGD. Specifically, problem (32) is transformed to (50) using the RS property. After that, CM-PAGD is employed to solve (50). The computational complexity of RS CM-PAGD is $\mathcal{O}(K^2 L + GK^3 \log(\epsilon_1^{-1}) \log(\epsilon_2^{-1}))$.
- **X CM-PAGD**: This is the algorithm we proposed based on the low dimensional beamforming structure discovered in (22)/(23)/(25)/(27) and CM-PAGD. Specifically, problem (32) is first transformed based on

TABLE I: Weighted Sum Rate (bps/Hz) Versus Transmit SNR (dB) Comparison among Different Strategies.

SNR	-10	-5	0	5	10	15	20	25	30
standard CM	0.5188	1.2833	2.6875	4.7814	7.4543	10.5215	13.7879	17.1312	20.3602
CM-PAGD	0.5190	1.2832	2.6854	4.7792	7.4536	10.5143	13.7855	17.1169	20.3101
CM-SA	0.5173	1.2787	2.6758	4.7473	7.3766	10.3571	13.3432	16.4204	19.5964
CM-LSE	0.5054	1.2645	2.6717	4.7515	7.4074	10.4447	13.4231	16.6817	19.8555
RS CM-PAGD	0.5190	1.2832	2.6854	4.7792	7.4536	10.5143	13.7854	17.1266	20.4048

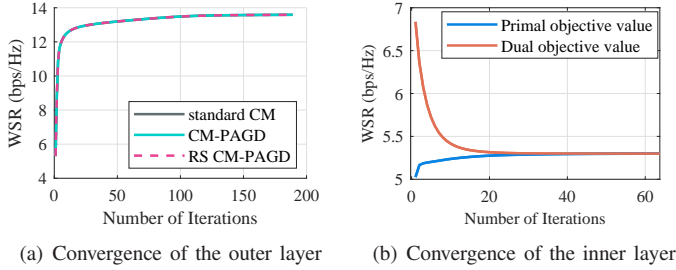


Fig. 1: Convergence of the proposed algorithms for a certain channel realization.

(22)/(23)/(25)/(27a)/(27b), respectively for the scenarios of X =MRT/ZF/RZF/MZF/MRZF. Subsequently, CM-PAGD is employed to solve the corresponding transformed problem. The computational complexity of X CM-PAGD is $\mathcal{O}(K^2L + GK_g^3 \log(\epsilon_1^{-1}) \log(\epsilon_2^{-1}))$.

All algorithms, excluding X CM-PAGD, aim at calculating sub-optimal beamforming solutions for the WSR problem (32). In contrast, X CM-PAGD algorithms are asymptotically optimal in different regimes. They notably reduce the computational complexity, but may lead to performance degradation in certain regimes.

C. Convergence of the Proposed Algorithms

We first check the convergence behavior of the standard CM algorithm, the proposed CM-PAGD and RS CM-PAGD algorithms. Both CM-PAGD and RS CM-PAGD have two iteration layers, namely, one outer layer for CM and one inner layer for PAGD. The convergence to both iteration layers is illustrated in Fig. 1(a) and Fig. 1(b), respectively. Fig. 1(a) shows the WSR performance of all three schemes as the number of iterations in the outer layer increases when $L = 16$, SNR=20dB. We would observe that the convergence path of the proposed CM-PAGD and RS CM-PAGD nearly overlap with the standard CM algorithm. This is because the convex surrogate problem (39c) is optimally solved by the derived optimal beamforming solution structure (43) together with the PAGD algorithm that successfully calculates the Lagrange dual variables. Fig. 1(b) illustrates the WSR versus the number of iterations in the inner layer for both dual and primal problems. It is obviously that the duality gap between the primal and the dual objective values converges to zero when solving each subproblem (39c).

D. Comparison among the Sub-optimal Algorithms

Table. I shows the WSR performance of the five sub-optimal algorithms as the transmit SNR increases from -10dB to

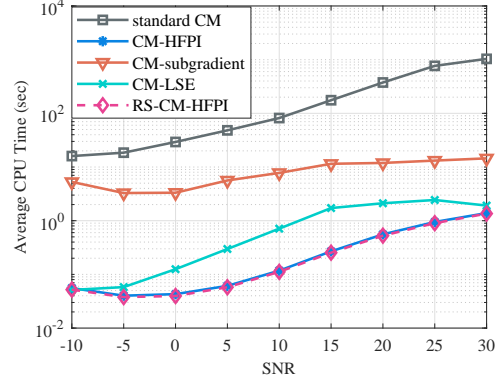


Fig. 2: Averaged CPU time versus the transmit SNR for different algorithms when $L = 16$, $G = 3$ and $K_G = 4$.

30dB. The number of transmit antenna is fixed to $L = 16$. Notably, the proposed CM-PAGD and RS-PAGD algorithms solve the WSR problem effectively without any performance loss compared to the standard CM. In comparison, CM-SA and CM-LSE cause certain performance degradation especially when SNR is large. This is due to the fact that in the high SNR regime, the CM-SA algorithm is more prone to oscillate in the vicinity of the non-differentiable optimal point during the inner iteration. Additionally, the LSE approximation function introduces a larger approximation error for the CM-LSE algorithm under these conditions. Fig. 2 illustrates the corresponding average CPU time versus the transmit SNR. Compared with other baselines schemes, the proposed algorithms exhibit substantial reduction in average CPU time. Notably, CM-PAGD and RS CM-PAGD achieve at least a 99.65% time decrease over standard CM across all SNR regimes, highlighting their effectiveness in achieving excellent WSR performance with lower computational complexity. The CPU time consumption for CM-PAGD and RS CM-PAGD is comparable since the number of transmit antennas $L = 16$ is of the same order as the total number of users $K = 12$, resulting in a marginal CPU time reduction for RS CM-PAGD. Furthermore, despite the potential higher complexity per iteration for CM-PAGD and RS CM-PAGD compared to CM-SA and CM-LSE, they exhibit faster convergence rates since CM-SA and CM-LSE converge in the primal field, while PAGD converges in the dual field. More details about the differences between these two types of approaches can be found in [40].

Table. II shows the WSRs achieved by different algorithms versus the number of transmit antennas with transmit SNR=20dB, and Fig. 3 illustrates the corresponding average CPU time. Due to the exponentially increasing computational cost of the standard CM with number of transmit antennas, we ex-

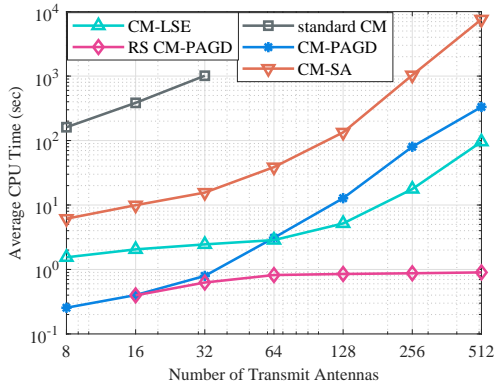


Fig. 3: Averaged CPU time versus the number of transmit antennas when $G = 3$, $K_G = 4$ and $\text{SNR} = 20\text{dB}$.

TABLE II: Weighted Sum Rate (bps/Hz) versus the Number of Transmit Antennas Comparison among Different Strategies.

L	16	32	64	128	256	512
standard CM	13.7879	16.6894	N/A	N/A	N/A	N/A
CM-PAGD	13.4855	16.4728	18.8373	20.8721	22.9418	24.9572
CM-SA	13.3432	16.0404	18.4644	20.7130	22.8966	25.0266
CM-LSE	13.4231	16.5445	18.6940	20.7340	22.8947	25.0205
RS CM-PAGD	13.7854	16.6882	18.8342	20.7431	22.8898	25.0221

clusively present its results for scenarios with 16 and 32 transmit antennas. Table. II shows that all algorithms demonstrate nearly identical WSR performance across varying numbers of transmit antennas. Notably, the proposed RS CM-PAGD attains such excellent WSR performance while significantly reducing computational time. Its computational time is not proportional to the number of transmit antennas. This substantial decrease in computational complexity for XL-MIMO transceiver design marks the proposed X CM-PAGD as a promising algorithm for 6G.

E. Comparison for Asymptotic Optimal Algorithms

Fig. 4 shows the WSR versus SNR comparison among different X CM-PAGD algorithms ($X = \text{MRT/ZF/RZF/MZF/MRZF}$) and RS CM-PAGD when the number of transmit antennas is $L = 16$. It is evident that MRT achieves near optimal performance in the low SNR regime (i.e., SNR from -10 dB to 0 dB), while MZF and MRZF achieve asymptotically optimal performance in the high SNR regime (i.e., SNR is larger than 20 dB). The numerical results align with the theoretical analysis in Section III. Also, it is observed that the classical ZF and RZF beamforming designs attain obvious performance loss compared to the near-optimal solution especially in the high SNR regime. This contrasts with the results in the unicast-only transmission [24], where ZF and RZF achieve near optimal performance. This is due to the distinct relations among user channels in the multi-group multicast communication, as discussed in Remark 2.

Fig. 5 illustrates the WSR versus the number of transmit antennas when $\text{SNR} = 20\text{dB}$. As the number of transmit antennas increases exponentially, RS, ZF, RZF, and MRZF all achieve asymptotically optimal WSR performance. In contrast, MRT exhibits relatively poor WSR performance due to

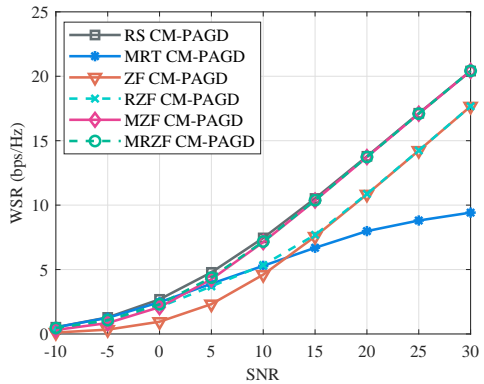


Fig. 4: WSR versus the transmit SNR, when $L = 16$, $G = 3$ and $K_G = 4$.

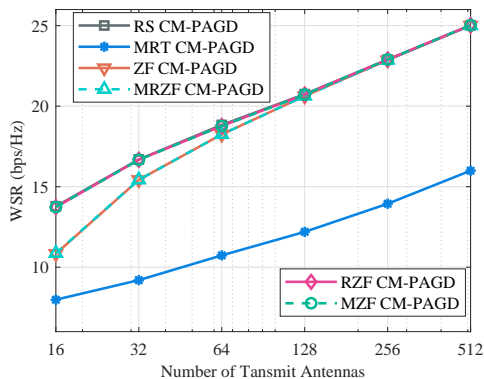


Fig. 5: WSR versus the number transmit antennas, when $G = 3$, $K_G = 4$ and $\text{SNR} = 20$ dB.

the asymptotic channel orthogonality. It suffers from severe performance degradation due to the presence of inter-group interference.

VI. CONCLUSION

In this study, we analyze the optimal and low-dimensional beamforming structures for a downlink multi-antenna multi-group multicast transmission network. Specifically, by leveraging the KKT conditions and SIT duality, we identify the optimal multi-group multicast beamforming structure for a general utility function-based maximization problem that embraces the WSR and MMF problems as special cases. This structure reveals valuable insights behind the multi-group multicast beamforming design, and inspires us to discover inherent low dimensional beamforming structures that are asymptotically optimal in various regimes of transmit SNR or the number of transmit antennas. These appealing beamforming structures provide guideline to efficient beamforming design for multi-group multicast transmission. Specially, we consider a special problem when the general utility function is the WSR. By exploiting the optimal beamforming structure, we propose an efficient optimization toolbox-free algorithm based on the CM framework and the proposed PAGD algorithm to solve the problem. We further exploit the low dimensional beamforming structures, and propose RS and MRT/ZF/RZF/MZF/MRZF based beamforming algorithms to further reduce the compu-

tational complexity. Numerical results demonstrate that these proposed algorithms achieve near-optimal performance while significantly reducing the computational complexity compared to the baseline schemes. They emerge as promising algorithms for ultra-massive MIMO applications in 6G.

The developed algorithms are not limited to solving WSR problems, they can be easily extended to other utility functions-based optimization problems, such MMF and energy efficiency. Additionally, as the proposed PAGD algorithm effectively addresses the non-smooth property introduced in the multicast rate expressions, it can be easily extended to solve the problems of power domain non-orthogonal multiple access (PD-NOMA) and rate splitting multiple access (RSMA). This is due to the similarity between the rate expressions of the streams to be decoded by multiple users in PD-NOMA (and RSMA) and the multicast rate expressions from a mathematical perspective.

REFERENCES

- [1] N. Sidiropoulos, T. Davidson, and Z.-Q. Luo, "Transmit beamforming for physical-layer multicasting," *IEEE Trans. Signal Process.*, vol. 54, no. 6, pp. 2239–2251, 2006.
- [2] H. Lu, Y. Zeng, C. You, Y. Han, J. Zhang, Z. Wang, Z. Dong, S. Jin, C.-X. Wang, T. Jiang *et al.*, "A tutorial on near-field XL-MIMO communications towards 6G," *arXiv preprint arXiv:2310.11044*, 2023.
- [3] C. Lu and Y.-F. Liu, "An efficient global algorithm for single-group multicast beamforming," *IEEE Trans. Signal Process.*, vol. 65, no. 14, pp. 3761–3774, 2017.
- [4] E. Karipidis, N. D. Sidiropoulos, and Z.-Q. Luo, "Quality of service and max-min fair transmit beamforming to multiple cochannel multicast groups," *IEEE Trans. Signal Process.*, vol. 56, no. 3, pp. 1268–1279, 2008.
- [5] T.-H. Chang, Z.-Q. Luo, and C.-Y. Chi, "Approximation bounds for semidefinite relaxation of max-min-fair multicast transmit beamforming problem," *IEEE Trans. Signal Process.*, vol. 56, no. 8, pp. 3932–3943, 2008.
- [6] Z. Xiang, M. Tao, and X. Wang, "Coordinated multicast beamforming in multicell networks," *IEEE Trans. Wireless Commun.*, vol. 12, no. 1, pp. 12–21, 2012.
- [7] D. Christopoulos, S. Chatzinotas, and B. Ottersten, "Weighted fair multicast multigroup beamforming under per-antenna power constraints," *IEEE Trans. Signal Process.*, vol. 62, no. 19, pp. 5132–5142, 2014.
- [8] L.-N. Tran, M. F. Hanif, and M. Juntti, "A conic quadratic programming approach to physical layer multicasting for large-scale antenna arrays," *IEEE Signal Process Lett.*, vol. 21, no. 1, pp. 114–117, 2013.
- [9] D. Christopoulos, S. Chatzinotas, and B. Ottersten, "Multicast multigroup beamforming for per-antenna power constrained large-scale arrays," in *Proc. IEEE Int Workshop Signal Process. Advances Wireless Commun.*, 2015, pp. 271–275.
- [10] G. Scutari, F. Facchinei, L. Lampariello, S. Sardellitti, and P. Song, "Parallel and distributed methods for constrained nonconvex optimization-part II: Applications in communications and machine learning," *IEEE Trans. Signal Process.*, vol. 65, no. 8, pp. 1945–1960, 2016.
- [11] L. Yin and B. Clerckx, "Rate-splitting multiple access for multigroup multicast and multibeam satellite systems," *IEEE Trans. Commun.*, vol. 69, no. 2, pp. 976–990, 2020.
- [12] —, "Rate-splitting multiple access for satellite-terrestrial integrated networks: Benefits of coordination and cooperation," *IEEE Trans. Wireless Commun.*, vol. 22, no. 1, pp. 317–332, 2022.
- [13] J. Zhou, Y. Sun, R. Chen, and C. Tellambura, "Rate splitting multiple access for multigroup multicast beamforming in cache-enabled C-RAN," *IEEE Trans. Veh. Technol.*, vol. 70, no. 12, pp. 12 758–12 770, 2021.
- [14] W. Wang, L. Gao, R. Ding, J. Lei, L. You, C. A. Chan, and X. Gao, "Resource efficiency optimization for robust beamforming in multi-beam satellite communications," *IEEE Trans. Veh. Technol.*, vol. 70, no. 7, pp. 6958–6968, 2021.
- [15] G. Zhou, C. Pan, H. Ren, K. Wang, and A. Nallanathan, "Intelligent reflecting surface aided multigroup multicast MISO communication systems," *IEEE Trans. Signal Process.*, vol. 68, pp. 3236–3251, 2020.
- [16] Z. Li, S. Wang, M. Wen, and Y.-C. Wu, "Secure multicast energy-efficiency maximization with massive RISs and uncertain CSI: First-order algorithms and convergence analysis," *IEEE Trans. Wireless Commun.*, vol. 21, no. 9, pp. 6818–6833, 2022.
- [17] Z. Zhang, Z. Zhao, K. Shen, D. P. Palomar, and W. Yu, "Discerning and enhancing the weighted sum-rate maximization algorithms in communications," *arXiv preprint arXiv:2311.04546*, 2023.
- [18] M. Grant and S. Boyd, "CVX: Matlab software for disciplined convex programming, version 2.1," <http://cvxr.com/cvx>, Mar. 2014.
- [19] E. Chen and M. Tao, "ADMM-based fast algorithm for multi-group multicast beamforming in large-scale wireless systems," *IEEE Trans. Commun.*, vol. 65, no. 6, pp. 2685–2698, 2017.
- [20] C. Zhang, M. Dong, and B. Liang, "Ultra-low-complexity algorithms with structurally optimal multi-group multicast beamforming in large-scale systems," *IEEE Trans. Signal Process.*, vol. 71, pp. 1626–1641, 2023.
- [21] H. B. Mahmoodi, B. Gouda, M. Salehi, and A. Tölli, "Low-complexity multicast beamforming for multi-stream multi-group communications," in *Proc. IEEE Global Commun. Conf. (GLOBECOM)*, 2021, pp. 01–06.
- [22] M. Sadeghi, L. Sanguinetti, R. Couillet, and C. Yuen, "Reducing the computational complexity of multicasting in large-scale antenna systems," *IEEE Trans. Wireless Commun.*, vol. 16, no. 5, pp. 2963–2975, 2017.
- [23] J. Yu and M. Dong, "Low-complexity weighted MRT multicast beamforming in massive MIMO cellular networks," in *Proc. IEEE Int. Conf. Acoust., Speech, Signal Process. (ICASSP)*. IEEE, 2018, pp. 3849–3853.
- [24] E. Bjornson, M. Bengtsson, and B. Ottersten, "Optimal multiuser transmit beamforming: A difficult problem with a simple solution structure [lecture notes]," *IEEE Signal Process Mag.*, vol. 31, no. 4, pp. 142–148, Jul. 2014.
- [25] M. Dong and Q. Wang, "Multi-group multicast beamforming: Optimal structure and efficient algorithms," *IEEE Trans. Signal Process.*, vol. 68, pp. 3738–3753, May. 2020.
- [26] T. Fang and Y. Mao, "Optimal beamforming structure for rate splitting multiple access," *arXiv preprint arXiv:2309.10342*, 2023.
- [27] C. Zhang, M. Dong, and B. Liang, "Fast first-order algorithm for large-scale max-min fair multi-group multicast beamforming," *IEEE Wireless Commun. Lett.*, vol. 11, no. 8, pp. 1560–1564, 2022.
- [28] S. Mohammadi, M. Dong, and S. ShahbazPanahi, "Fast algorithm for joint unicast and multicast beamforming for large-scale massive MIMO," *IEEE Trans. Signal Process.*, vol. 70, pp. 5413–5428, 2022.
- [29] H. Tuy, "Robust solution of nonconvex global optimization problems," *J. Global Optim.*, vol. 32, pp. 307–323, 2005.
- [30] D. W. Peterson, "A review of constraint qualifications in finite-dimensional spaces," *SIAM Review*, vol. 15, no. 3, pp. 639–654, 1973.
- [31] B. Matthiesen and E. A. Jorswieck, "Efficient global optimal resource allocation in non-orthogonal interference networks," *IEEE Trans. Signal Process.*, vol. 67, no. 21, pp. 5612–5627, 2019.
- [32] B. Matthiesen, Y. Mao, A. Dekorsy, P. Popovski, and B. Clerckx, "Globally optimal spectrum- and energy-efficient beamforming for rate splitting multiple access," *IEEE Trans. Signal Process.*, vol. 70, pp. 5025–5040, Oct. 2022.
- [33] C. B. Peel, B. M. Hochwald, and A. L. Swindlehurst, "A vector-perturbation technique for near-capacity multi-antenna multiuser communication-part I: channel inversion and regularization," *IEEE Trans. Commun.*, vol. 53, no. 1, pp. 195–202, 2005.
- [34] M. Asghari, A. M. Fathollahi-Fard, S. Mirzapour Al-E-Hashemi, and M. A. Dulebenets, "Transformation and linearization techniques in optimization: A state-of-the-art survey," *Mathematics*, vol. 10, no. 2, p. 283, 2022.
- [35] S. Boyd, L. Xiao, and A. Mutapcic, "Subgradient methods," *lecture notes of EE392o, Stanford University, Autumn Quarter*, 2003.
- [36] S. Xu, "Smoothing method for minimax problems," *Comput. Optim. Appl.*, vol. 20, no. 3, pp. 267–279, 2001.
- [37] X. Zhao, S. Lu, Q. Shi, and Z.-Q. Luo, "Rethinking WMMSE: Can its complexity scale linearly with the number of BS antennas?" *IEEE Trans. Signal Process.*, vol. 71, pp. 433–446, 2023.
- [38] M. Journée, Y. Nesterov, P. Richtárik, and R. Sepulchre, "Generalized power method for sparse principal component analysis," *J. Mach. Learn. Res.*, vol. 11, no. 2, 2010.
- [39] Y. Sun, P. Babu, and D. P. Palomar, "Majorization-minimization algorithms in signal processing, communications, and machine learning," *IEEE Trans. Signal Process.*, vol. 65, no. 3, pp. 794–816, 2017.
- [40] S. Boyd, S. P. Boyd, and L. Vandenberghe, *Convex optimization*. Cambridge university press, 2004.